Chapter 2
TeO_2 Bolometric Detectors for 0νDBD Search

The neutrinoless double beta decay is a very rare process, and the experimental search demands a large amount of mass operating in low background conditions. Current limits on the half-life of this process range between 10^{21} and 10^{25} years, depending on the source isotope. The most promising detectors are probably bolometers, and next generation experiments will improve the sensitivity to the half-life by two orders of magnitude with respect to the present limits. CUORE [1, 2] will be a ton scale experiment that will probe neutrinoless double beta decay in ^{130}Te using TeO_2 bolometers.

The use of bolometric detectors for the search of neutrinoless double beta decay was proposed by Fiorini in 1984 [3]. The successful operation of a 340 g Tellurium dioxide crystal was followed by the construction of a detector array composed by 20 crystals, for a total mass of 6.8 kg of TeO_2 [4]. A further mass increase was obtained with the recently completed CUORICINO experiment [5]. Operated in the Laboratori Nazionali del Gran Sasso in the years 2003–2008, CUORICINO was composed by a tower of 62 TeO_2 bolometers, with a total mass of $\sim$41 kg. At present the CUORICINO result represents one of the most competitive limits, comparable with the ones obtained with Germanium detectors. The excellent performance obtained with CUORICINO demonstrates the feasibility of CUORE, aiming at the investigation of the effective neutrino mass in the inverted hierarchy range.

In this chapter the TeO_2 bolometric detectors will be presented.

2.1 Bolometric Detectors

Bolometers are calorimeters working at low temperatures in which the energy of particle interactions is converted into phonons and measured via temperature variation. Conventional techniques for energy deposition measurements are based on the detection of the energy released in the form of ionization and excitation of the atoms in the detector. Unfortunately, the amount of energy lost in channels different from the detected ones is quite large. Most of the energy is converted in phonon excitations

M. Vignati, *Model of the Response Function of CUORE Bolometers*, Springer Theses,
DOI: 10.1007/978-94-007-1232-4_2,

inside the detector and is not measured. Thermal detectors on the other hand measure the portion of the deposited energy converted into phonons and guarantee a better intrinsic energy resolution. Nevertheless they are slow detectors so that they are suitable only for experiments working at low rates. Bolometers consist of two main components: an energy absorber, where particles deposit their energy, and a sensor, which converts the excitations produced by the particle into a signal (see Fig. 2.1).

2.1.1 The Energy Absorber

The absorber can be roughly sketched as a heat capacitance C connected to an heat bath through a conductance K. The temperature variation induced by a deposit of energy E, assuming that C does not depend on temperature, is:

$$\Delta T = \frac{E}{C}. \tag{2.1}$$

The absorbed heat then flows trough the conductance until an equilibrium condition with the heat sink is reached:

$$\Delta T(t) = \frac{E}{C}\exp\left(-\frac{t}{\tau}\right) \tag{2.2}$$

where $\tau = C/K$ is the time constant of the bolometer. With these simple considerations, it is clear that to obtain big and fast signals the capacitance of the absorber must be small. This requirement can be fulfilled only operating at cryogenic temperatures, between 10 and 100 mK.

The specific heat of a material at low temperatures is the sum of the lattice and the electron specific heats:

$$c(T) = c_l(T) + c_e(T) \tag{2.3}$$

The lattice specific heat is described by the Debye law:

$$c_l(T) = \frac{12}{5}\pi^4 N_a k_B \left(\frac{T}{\Theta_D}\right)^3 \quad T < \Theta_D \tag{2.4}$$

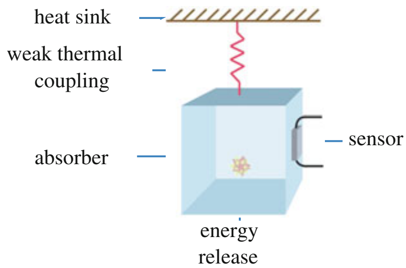

Fig. 2.1 Schematic representation of a bolometric detector: an absorber is connected to a heat sink through a weak thermal coupling, a sensor for signal readout is attached to the absorber

where N_a, k_B and Θ_D are the Avogadro number, the Boltzmann constant and the Debye temperature, respectively. In metals the specific heat of the electrons is:

$$c_e(T) = \frac{ZR}{\Theta_D}\pi^2\frac{T}{\Theta_F} \tag{2.5}$$

where Z, R and Θ_F are the number of conduction electrons, the gas constant and the Fermi temperature, respectively. Given the different temperature dependence of c_l and c_e, the electron specific heat dominates at low temperatures. Dielectric and diamagnetic materials, lacking in electron contribution, have then lower capacitance and are preferred. Particles can interact with the absorber by scattering on nuclei or on electrons, in both cases the energy is finally converted into phonons. When particles interact with nuclei the released energy produces vibrational excitations but may also produce structural damages of the lattice, where the energy can be stored. If this energy is not converted into phonons, the statistical fluctuation of the number of produced defects can worsen the energy resolution. In a very simplified model in which all the thermal phonons are detected, a rough estimate of the energy resolution can be derived. The thermodynamic equilibrium between the absorber and the heat sink is hold by a continuum exchange of phonons trough the conductance K. The fluctuation of the number of phonons in the absorber produces a temperature variation that in turns affects the energy resolution. These fluctuations can be computed as follows.

The energy E in the absorber is:

$$E = C(T) \cdot T \tag{2.6}$$

or in terms of the energy of each phonon $\varepsilon = k_B T$:

$$E = N \cdot \varepsilon. \tag{2.7}$$

Assuming that the number of phonons obeys the Poisson statistics, the energy fluctuation is:

$$\Delta E = \Delta N \cdot \varepsilon = \sqrt{k_B C(T) T^2}. \tag{2.8}$$

It should be stressed that, at least for CUORE bolometers, the thermodynamic fluctuations give a negligible contribution to the energy resolution. From the above expression, using typical values of CUORE bolometers ($C = 10^{-9}$ J/K, $T = 10$ mK), a resolution of ~ 10 eV is predicted, that is well below the measured resolution (few keV). The thermodynamic limit can be obtained only when the statistical fluctuations of the physical processes coming before the thermalization are negligible, when the temperature of the heat sink is constant enough, and when the noise of the detector is minimized (see Sect. 2.6).

2.1.2 The Choice of TeO_2

CUORE uses TeO_2 crystals as absorbers. The use of TeO_2 is motivated by various reasons, some of them related to the 0νDBD candidate isotope (^{130}Te) and others related to the cryogenic properties of the material. Double beta decay of ^{130}Te occurs through the transition:

$$^{130}\mathrm{Te} \rightarrow ^{130}\mathrm{Xe} + 2e^- + (2\bar{\nu}). \tag{2.9}$$

The most striking feature of ^{130}Te compared to other 0νDBD isotopes is the high natural abundance (see Table 1.3). Compared to other materials that usually need to be enriched, the abundance of ^{130}Te allows to build an experiment with natural Tellurium. This is an advantage both in terms of costs and material cleanliness, as enrichment procedures often introduce radioactive contaminations. The transition energy of ^{130}Te ($Q_{\beta\beta} = 2527.0 \pm 0.3$ keV [6]) is not very high. It has been shown in Sect. 1.4 that experiments using isotopes with Q-values above 2615 keV are affected by a much lower radioactivity background. However, this transition energy happens to be situated between the peak and the Compton edge of the 2615 keV line of ^{208}Tl which leaves a clean window to look for the signal.

The possibility to use pure Tellurium crystals as absorbers was taken into account, but it was ruled out mainly because of the poor mechanical properties at low temperatures. Stresses caused by the thermal contractions revealed to produce excessive damages on pure Te crystals. TeO_2 has instead a good mechanical behavior, and has an higher Debye temperature, implying lower specific heat and thus a higher sensitivity to thermal pulses.

2.1.3 The Sensor

The phonon sensor is usually a thermistor, a resistive device that converts temperature variations into resistance variations. There are basically two types of thermistors, Transition Edge Thermistors (TES) and Semiconductor Thermistors (ST). TES are superconducting films kept at the critical temperature, they have a rather fast response ($\sim \mu$s) but can only work in a narrow range of temperatures. On the other hand ST have a slower response ($\sim$ms) but can be used in a wider range of temperatures. A parameter characterizing the sensor is the logarithmic sensitivity η:

$$\eta = \left| \frac{d\log R(T)}{d\log T} \right|. \tag{2.10}$$

The above expression implies that (apart signs):

$$\frac{dR}{R} = \eta \frac{dT}{T} \tag{2.11}$$

where it is evident that the larger is η the higher is the response of the device. Typical values of η are 10 for ST and 100 for TES. Despite the lower sensitivity, ST have been preferred for CUORE bolometers because of their wider range of operating temperature. In the following, the operating principles of semiconductor thermistors will be presented.

Semiconductors are covalent solids that behave as insulators because the valence band is full and the conduction band is empty, nevertheless the energy gap between valence and conduction band is smaller than 2 eV. The conduction can happen only with an activation energy greater than the energy gap. Since at room temperature $kT \simeq 0.025$ eV, the conduction can only happen at higher temperatures. If instead the semiconductor lattice has impurities (extrinsic or doped semiconductors), then new energy levels are introduced slightly above the valence band or below the conduction band, depending on the type of atoms inserted. With this technique the conduction can also happen at lower temperatures. The dopant concentration determines the behavior of the solid and there is a critical concentration that characterizes the transition from metal to insulator. The region near this concentration is named metal-insulator transition region (MIT) [7], where the material resistivity exhibits a strong dependence on the temperature.

At temperatures lower than 10 K the conduction is dominated by the migration of the charge carries between impurity sites. In this situation electrons are not localized and the conduction happens when an electron jumps from a donor site to another, without using the conduction band (*hopping mechanism*). This migration is due to the tunnelling through the potential barrier separating the two dopant sites and it is activated by phonons (see Fig. 2.2). At even lower temperature, the energy of the phonons that are responsible for the conduction mechanism is low, and charge carriers migrate also to far impurity sites with free energy levels that are close to the Fermi energy. In this conduction regime, called Variable Range Hopping [8] (VRH), the concentration of minority charge carriers determines the density of states close to the Fermi level. The MIT is set not only varying the concentration of dopant but also varying the ratio of acceptor and donor concentrations.

In the VRH conduction regime the resistivity dependence on temperature is described by the law:

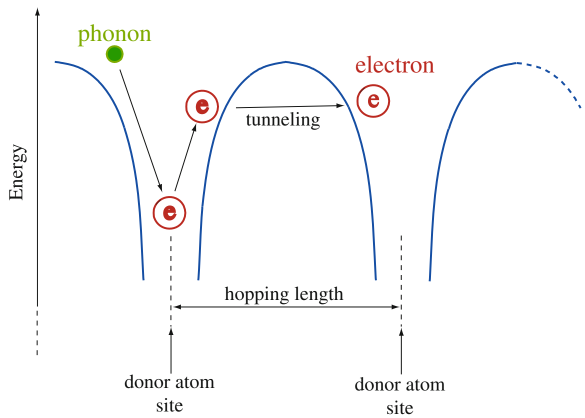

Fig. 2.2 Schematic representation of the hopping conduction mechanism

$$\rho(T) = \rho_0 \exp\left(\frac{T_0}{T}\right)^\gamma \tag{2.12}$$

where ρ_0, T_0 depend on the doping concentration and $\gamma = 1/2$. The expression of the logarithmic sensitivity can be easily derived from the above equation using (2.10):

$$\eta = \gamma\left(\frac{T_0}{T}\right)^\gamma. \tag{2.13}$$

2.1.4 NTD-Ge Thermistors

The thermal sensor used in CUORICINO and CUORE bolometers is a Neutron Transmutation Doped (NTD)germanium thermistor operating in the VRH regime [9]. Melt-doped Ge crystals cannot achieve the necessary uniformity due to the effect of dopant segregation. The only technique available for producing uniform doping is NTD: Ge wafers are bombarded with thermal neutron beams that, inducing nuclear reactions, create donor (As and Se) and acceptor (Ga) impurities. The natural abundances of Germanium are such that this doping technique allows to obtain the right dopant concentration, which determines the sensor performances. Wafers are then cut into pieces, each of them is a thermistor and its resistance can be expressed as:

$$R = R_0 \exp\left(\frac{T_0}{T}\right)^\gamma \tag{2.14}$$

where R_0 depends on the geometry and is roughly $R_0 = \rho_0 l/S$, being l and S the length and the section of the piece, respectively. The parameters R_0, T_0 and γ are determined experimentally. The measurement is made coupling the sensor to a low temperature heat sink using an high conductivity epoxy, so that the electrothermal feedback is negligible (see next section). The heat sink temperature is then varied (15–50 mK) while a steady current flows through the thermistor. Using a calibrated thermometer the parameters can be extracted from a fit to the $R(T)$ characteristic. Typical parameters of CUORE NTDs are:

$$R_0 = 1.15\,\Omega, \quad T_0 = 3.35\,\text{K} \quad \text{and} \quad \gamma = 1/2 \tag{2.15}$$

Using these values we can calculate the static resistance (R_S) at the working temperature $T_S = 10$ mK to be approximately 100 MΩ.

2.2 Bolometer Operation

To measure the resistance variation the thermistor is biased with the circuit shown in Fig. 2.3a. A bias voltage V_B is produced by a voltage generator closed on a load

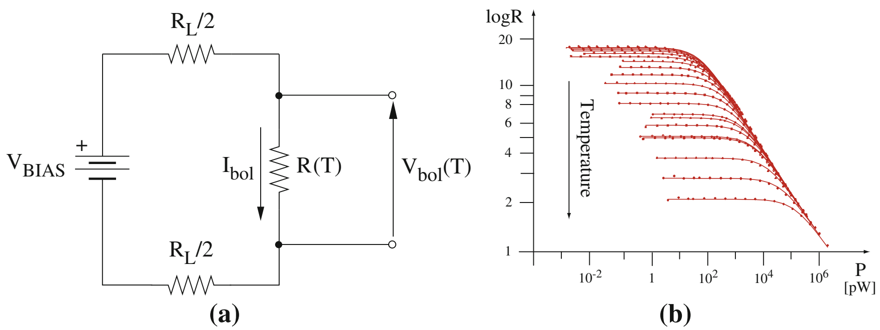

Fig. 2.3 Picture **a** shows the electric scheme of the bias circuit used for thermistor readout. Picture **b** shows the dependence of the resistance on the power dissipation for various values of the base temperature. Curves with lower resistance at $P = 0$ correspond to higher base temperatures

resistor that is put in series with the thermistor. The load resistance R_L is chosen much higher than the thermistor resistance R so that the current in the circuit I is constant and the voltage across the thermistor V_{bol} is proportional to R:

$$V_{\text{bol}}(T) = I \cdot R(T). \tag{2.16}$$

This current produces a power dissipation $P = VI$ that in turns heat the thermistor decreasing its resistance, this phenomenon is known as "electrothermal feedback". In static conditions the thermistor temperature T_S is

$$T_S = T_{hs} + \frac{P}{K} \tag{2.17}$$

where T_{hs} is the temperature of the heat sink and K is the conductance to it. The $R - P$ dependence is depicted in Fig. 2.3b. The electrothermal feedback makes the $I - V$ relation deviate from linearity and leads to a nonohmic behavior (see Fig. 2.4a). Increasing the bias current the slope of the curve increases until it crosses the so called inversion point (IP) and then decreases. In static conditions the thermistor electric and thermal parameters are described by a point on the load curve.

When particles release an amount of energy E in the absorber the voltage across the thermistor varies leading to a signal. A rough estimate of the voltage increase is:

$$\Delta V = \eta V \frac{\Delta T}{T_S} = \eta \sqrt{P \cdot R_S} \frac{E}{C T_S} \tag{2.18}$$

where R_S is the static resistance and we used $R_L \gg R_S$. This expression vanishes both for $P \to 0$ and $P \to \infty$ because the resistance vanishes at high temperatures, then a maximum signal amplitude must exists somewhere. If all the detector parameters were known, the optimal working point could be determined

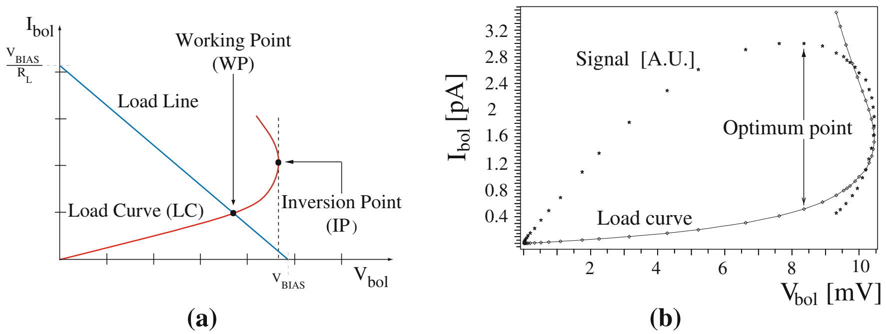

Fig. 2.4 Load curve of a semiconductor thermistor. In picture **a** the working point is determined by intersection of the sensor characteristic curve with the bias circuit load line. In picture **b** the load curve is shown together with the corresponding signal amplitude

analytically. Nevertheless not all the parameters are known and the working point has to be determined experimentally. The procedure consists in scanning the amplitude of a pulse of fixed energy varying the bias current, and selecting the point where the signal is maximum (see Fig. 2.4b).

2.3 Arrays of TeO_2 Bolometers

The single module is the elementary unit of arrays of TeO_2 detectors. Its components are: the absorber crystal of TeO_2 the NTD thermistor, the heater, the PTFE supports and the copper structure. The NTD-Ge thermistor is glued onto the TeO_2 crystals by nine spots of Araldit Rapid epoxy (diameter 0.5 mm, height 50 μ m). The crystal is held by PTFE supports in copper frames. The copper frames are connected to the mixing chamber of a dilution refrigerator that provides the base low temperature ($\sim$10 mK) to operate the bolometers. Heaters [10] are heavily doped silicon chips with a resistance between 50 and 100 kΩ. They are glued to the crystals and used as Joule heaters to inject a controllable energy to emulate the effect produced by particles for calibration purposes (see Sect. 4.1). The single modules are usually packed into floors that in turn are piled up to form a tower. As an example, the CUORICINO tower is represented in Fig. 2.5a.

2.4 Cryogenic Setups

To reach the temperature of 10 mK the TeO_2 bolometric experiments need a cryogenic setup. Two cryogenic setups were installed in the eighties at Laboratori Nazionali del Gran Sasso (LNGS) in Italy. The first one, hosted in the hall A of the

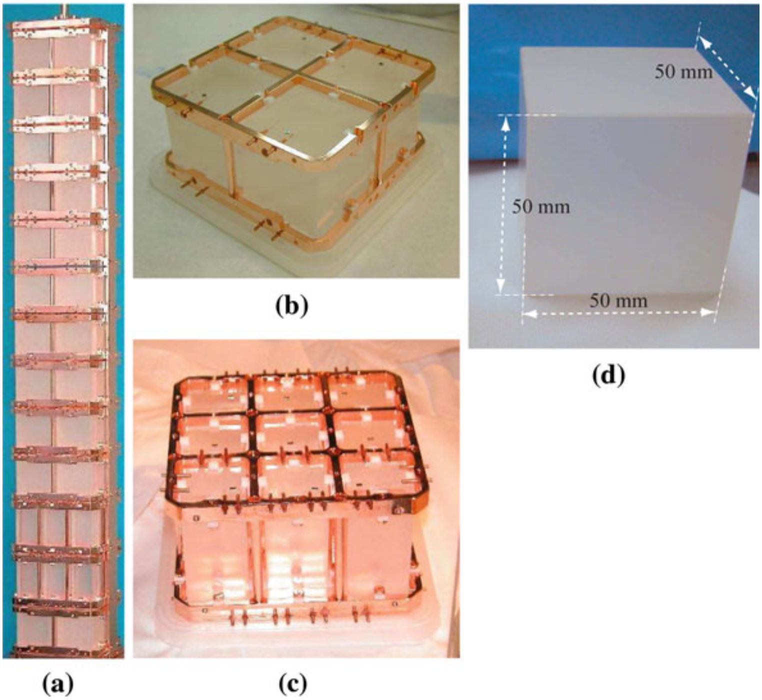

Fig. 2.5 Pictures of the CUORICINO detector. **a** the tower. **b** one of the eleven floors composed by four crystals. **c** one of the two floors composed by nine crystals. **d** A $5 \times 5 \times 5$ cm^3 TeO_2 crystal

laboratory, was used for CUORICINO and is now used for R&D activities. The second one, hosted in the C hall, has been always dedicated to R&D activities for CUORE. Both of them are dilution refrigerators housed inside Faraday cages to suppress electromagnetic interferences. The experimental volume in the hall A cryostat is about 16 l while in the hall C one is less then a third. The dilution refrigerators are equipped with heavy shields against environmental radioactivity. In particular, the hall A one is shielded with two layers of lead of 10 cm minimum thickness each. The outer layer is made of commercial low radioactivity lead, while the internal one is made with special lead with a ^{210}Pb contamination of 16 Bq/kg (see Fig. 2.6). The external lead shields are surrounded by an air-tight box flushed with fresh nitrogen from a dedicated evaporator to avoid radon contamination of the gas close to the cryostat. In order to shield the detectors against the unavoidable radioactive contamination from some fundamental components of the dilution refrigerator, thick layers of Roman lead are placed inside the cryostat just around the detectors. A borated polyethylene neutron shield, 10 cm thick, was added in 2001 to the hall A cryostat.

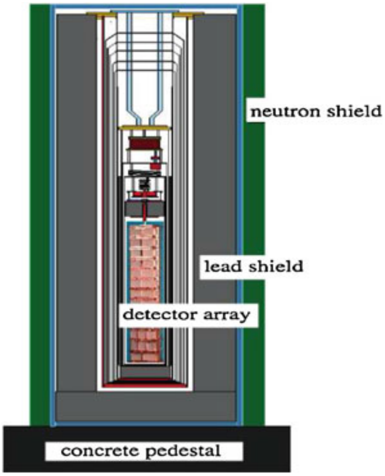

Fig. 2.6 Sketch of the CUORICINO apparatus showing the tower hanging from the mixing chamber of the dilution refrigerator and the detector shields

2.5 Signal Readout

The bolometers are connected to the electronics at room temperature through a set of wires. After coming out from the single module, the signal runs along the tower over a twisted pair of wires, until it reaches the mixing chamber. From this point on, the signal is delivered over a pair of twisted coaxial cables that passing through several thermalization stages reach the exterior of the cryostat. These wires are made of constantan, an electric conductor that has the rare property of not conducting heat. The cryostat is finally plugged to the front-end (FE) electronic boards through a set of Fisher connectors.

The FE boards contain the bias voltage generator, the load resistors and the amplification stages, and all the parameters are remotely programmable [11]. As stated in Sect. 2.2 the load resistors must be large compared to the sensor resistance; since the typical thermistor resistance R_S is of order 100 MΩ at 10 mK, their value is 27 GΩ each. The bias voltage V_B can be set in the range 0–10 V and for a typical bias $V_B = 5$ V the output voltage of the thermistor when no energy is released in the crystal is:

$$V_{R_S} = V_B \frac{R_S}{R_S + R_L} \simeq 10\,\text{mV}. \tag{2.19}$$

where R_L represent the series of the two load resistors. The signal observed when particles impinge on the detector leads to a voltage variation of about 200 μV/MeV that in turn is amplified. The gain (G) of the amplifier is adjusted to fit the energy region of interest into the ADC range with G ranging between 450 and 10,000 V/V. The drift current of the amplifier generates an offset voltage that summed to $V_{R_S} \cdot G$ can shift the signal out of the ADC range. To correct for this effect an additional offset is added to the output signal.

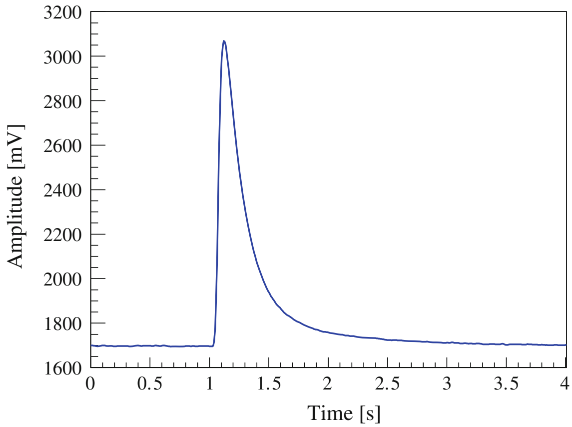

Fig. 2.7 Acquired signal generated by a 2615 keV γ particle

After the amplification and the offset correction the signal goes through an anti-aliasing six-pole Bessel Filter with an attenuation of 120 dB/decade and a programmable cutoff ranging between 8 and 20 Hz. Finally the signal is acquired by an ADC (range $[-10.5, 10.5]$ V, 18 bits) with a typical sampling period of 8 ms (125 Hz). Given the low event rate, it was possible to implement a software trigger. When a trigger is found the signal is recorded in a window of $\sim$3 s. In order to have an estimate of the bolometer temperature at the time of the pulse (see Sect. 4.1), about one second of baseline before the trigger is recorded, so that the total window is $\sim$4 s.

Triggered events are then written to disk for offline processing. A typical event generated by a 2,615 keV γ particle is shown in Fig. 2.7.

2.5.1 Measurement of the Static Resistance

The thermistor static resistance (R_S) is measured right after the detector cooling to estimate the working temperature of each detector. This parameter is also one of the ingredients of the model developed in the next chapters. In this section we describe the procedure to measure the value of R_S that is extracted from (2.19) by measuring V_{R_S}.

The voltage measured at the end of the readout chain is not only the amplified thermistor voltage, but contains also an unknown offset V_h generated by the amplifier itself and by the front-end board:

$$V = V_{R_S} G + V_h. \tag{2.20}$$

To cancel this contribution the thermistor is biased with an opposite voltage $-V_B$ so that V_{R_S} changes sign while V_h does not:

$$V^+ = V_B \frac{R_S}{R_S + R_L} G + V_h = V_{R_S} G + V_h \tag{2.21}$$

$$V^- = -V_B \frac{R_S}{R_S + R_L} G + V_h = -V_{R_S} G + V_h. \tag{2.22}$$

It is important to notice that the gain used during normal acquisition runs is almost always too high to contain both these voltages into the ADC range. The gain is therefore lowered to a smaller value G_S (where the S subscript is related to the R_S measurement). The voltage across the thermistor is then evaluated as:

$$V_{R_S} = \frac{V^+ - V^-}{2G_S} \tag{2.23}$$

and the corresponding resistance is:

$$R_S = \frac{R_L}{V_B/V_{R_S} - 1}. \tag{2.24}$$

2.6 Detector Noise

The thermodynamic fluctuations of the crystal described in Sect. 2.1.1 represent the ultimate noise source. In practical applications they give a negligible contribution compared to the noise coming from the electronics and the cryogenic apparatus. The first noise source are the load resistors (R_L). Every resistance R working at temperature T, in fact, generates a white noise due to the fluctuations of the charge carriers. For load resistors the noise spectral density can be expressed as:

$$\Delta V_L^2 = 4kT_{R_L} R_L \tag{2.25}$$

that on the output voltage of the bolometer becomes:

$$\Delta V_b^2 = \frac{\Delta V_L^2}{(R_L{}^2)} \left(\frac{R_S R_L}{R_S + R_L} \right)^2 \simeq 4kT \frac{R_S^2}{R_L}. \tag{2.26}$$

Using the detector typical parameters the above equation translates into a noise of order 300 eV rms. The second noise source are the preamplifiers, and is of three types: *series*, generated by the JFET resistances, having a value around 10 eV rms, *series 1/f* that amounts to 15 eV rms and *parallel shot*, that at room temperature amounts to 130 eV rms. To reduce this noise, load resistors and preamplifiers of some channels were housed in the cryostat at $\sim$110 K. This cold electronics setup however did not improve the resolution of the detector.

The last and dominant noise contribution comes from the vibrations of the cryogenic apparatus. These vibrations are transmitted to crystals and wires producing two different types of noise. The first is due to crystal vibrations that generate an energy dissipation that in turn changes the temperature. These temperature instabilities have a frequency spectrum similar to the signal one, and then they are the most dangerous source of noise. The second is due to wires vibrations that change the wire–wire capacitance and the wire–ground capacitance, generating the so called *microphonic* noise.

Quantifying the amount of vibrational noise is difficult, and it strictly depends on the cryogenic setup and on the detector assembly. These vibrations are partially reduced hanging the detector to the cryostat by means of a spring, and mechanically decoupling the cryostat from the outer environment.

2.7 CUORICINO and CUORE

The CUORICINO detector was a tower like structure. It was composed by eleven floors of four modules each ($5 \times 5 \times 5$ cm^3 crystals) and two additional floors of nine modules each ($3 \times 3 \times 6$ cm^3 crystals). The small crystals came from the previous MiDBD experiment while the big crystals were made explicitly for CUORICINO. Two of these smaller crystals were enriched in ^{130}Te and two were enriched in ^{128}Te. These crystals were designed to measure the DBD spectrum of ^{130}Te by subtracting the background seen in the crystals enriched in ^{128}Te. The result of this analysis was a measurement of the ^{130}Te DBD half-life of 6.1×10^{20} year [12].

The collected statistics was about $18\,\text{kg} \cdot \text{y}$ of ^{130}Te in 5 years of data taking. Part of this data ($11.83\,\text{kg} \cdot \text{y}$) have been analyzed assuming a Q-value of 2530 keV. The background rates in the 0νDBD region were 0.18 ± 0.01 counts/keV/kg/y for the $5 \times 5 \times 5$ crystals, and 0.20 ± 0.04 counts/keV/kg/y for the small crystals. The energy resolution was evaluated to be 7 and 12 keV FWHM for the big and the small crystals, respectively. The single-hit spectrum is shown in Fig. 2.8. The experiment was able to set a lower limit of 3.0×10^{24} y for the 0νDBD half life of ^{130}Te corresponding to $m_{\beta\beta} < 0.19$–0.68 eV, depending on the nuclear matrix element evaluation [13–16].

The CUORE detector will be made of 19 towers of 13 floors each, with four $5 \times 5 \times 5$ cm^3 crystals per floor (see Fig. 2.9). The goal of this experiment is to achieve sensitivity to the inverted neutrino mass hierarchy. By increasing the mass by a factor twenty, and reducing the background by a similar factor, the CUORE collaboration will improve the sensitivity to the ^{130}Te by a factor twenty. The detector will be hosted in the A Hall of LNGS, the same experimental hall of CUORICINO, the construction is scheduled for completion in 2013.

Now that the mass of the detector is fixed, the collaboration is mainly working on improving the resolution and the background of the detector. The target

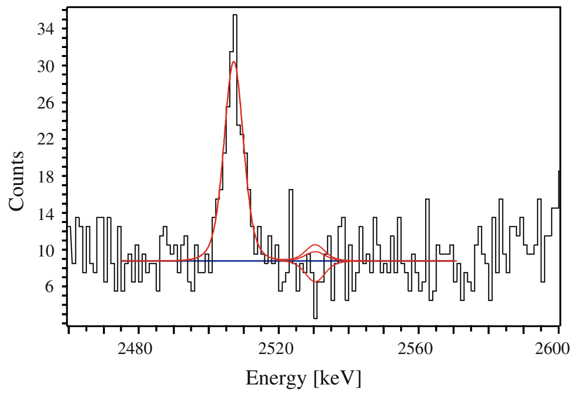

Fig. 2.8 Single hit background spectrum of CUORICINO. The peak at 2505 keV is produced by the two gamma's emitted in the beta decay of ^{60}Co. It is about 7σ away from the position where the 0νDBD peak is expected. The red lines represent the best fit to the number of 0νDBD events, 68 and 90% C.L. bounds

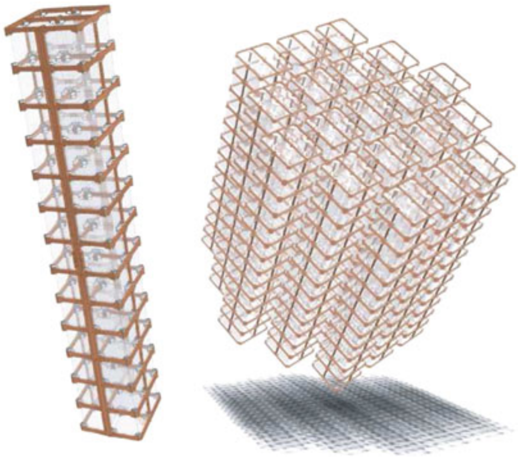

Fig. 2.9 CUORE detector array is roughly 19 times CUORICINO

resolution is 5 keV FWHM and will be realized reducing the detector noise. Given that the main noise contribution is generated by crystal vibrations, the new detector structure, known as "Gorla" configuration by the name of the proponent, includes a new design of the Teflon supports. These supports, thanks also to the tighter crystal size tolerances, clench the crystal reducing vibrations. The background coming from the cryostat and from the outside will be reduced including a thicker lead shield inside the cryostat. The background generated by radioactive contaminations of the copper structure is currently under study, and different cleaning techniques of the copper are being tested (see Sect. 5.1). In the hoped case, CUORE will have a background of 0.01 counts/keV/kg/y, corresponding to a half-life sensitivity of about 2.1×10^{26} y in 5 years (see Fig. 2.10).

The main technical efforts concern the construction of the cryostat and the calibration system. The detector will be cooled by a ^{3}He/^{4}He dilution refrigerator that is being especially designed for CUORE by Leiden Cryogenics and is sketched in Fig. 2.11.

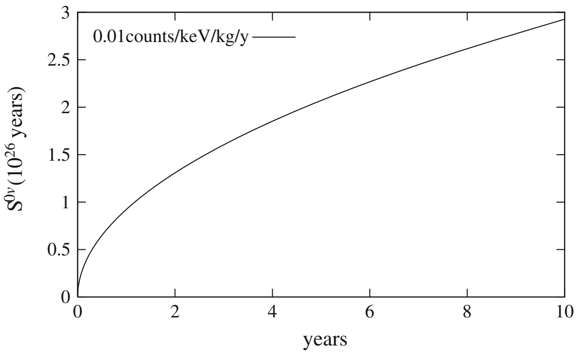

Fig. 2.10 CUORE sensitivity to the 0νDBD half-life assuming a background of 0.01 counts/keV/kg/y

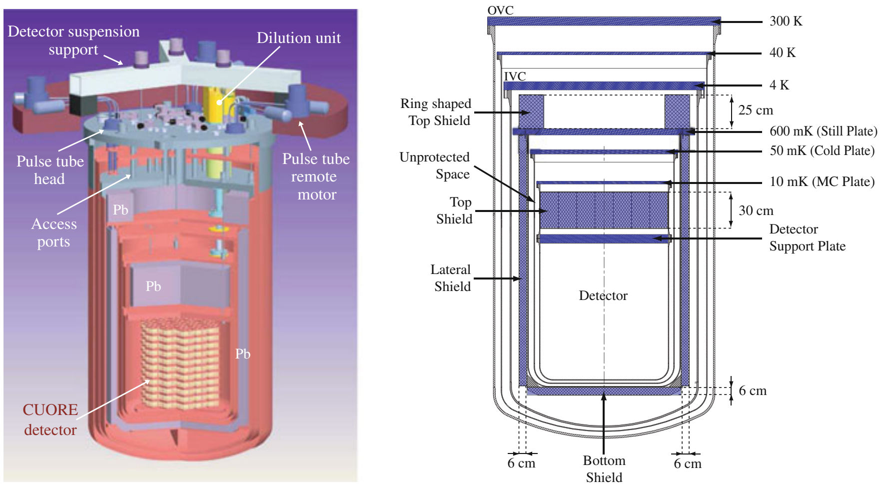

Fig. 2.11 CUORE cryostat and internal shieldings

Regarding CUORICINO, it was calibrated facing Thorium sources to the detector from the outside of the cryostat (see Sect. 4.4.1). The greater amount of TeO_2 in CUORE makes this technique not usable. If the detector were exposed to an external source, the innermost bolometers would experience a much lower rate of calibration events than the outermost. To solve this problem sources of different intensity could be used to calibrate at different times inner and outer bolometers. Given that this procedure should last at least a week, and given that the calibration is repeated every month, the live time of the experiment could be significantly reduced. An alternative option consists in inserting the sources between the towers, in the 10 mK environment. The system to lower and raise the sources is currently being developed, taking into account the radioactivity constraints and the time needed to thermalize the sources from 300 K to 10 mK, that even in this case could not be negligible.

References

1. Arnaboldi, C., et al.: Nucl. Instrum. Meth. A **518**, 775 (2004). doi:10.1016/j.nima.2003.07.067
2. Ardito, R., et al.: (2005)
3. Fiorini, E., Niinikoski, T.O.: Nucl. Instrum. Meth. A **224**, 83 (1984)
4. Alessandrello, A., et al.: Phys. Lett. B **486**, 13 (2000)
5. Arnaboldi, C., et al.: Phys. Rev. C **78**, 035502 (2008). doi:10.1103/PhysRevC.78.035502
6. Scielzo, N., et al.: Phys. Rev. C **80**(2), 025501 (2009)
7. Mott, N.F., Davies, J.H.: Philos. Mag. B **42**, 845 (1980)
8. Miller, A., Abrahams, E.: Phys. Rev. **120**, 745 (1960)
9. Itoh, K.M., et al.: Appl. Phys. Lett. **64**, 2121 (1994)
10. Arnaboldi, C., Pessina, G., Previtali, E.: IEEE Trans. Nucl. Sci. **50**, 979 (2003). doi: 10.1109/TNS.2003.815346
11. Arnaboldi, C., et al.: IEEE Trans. Nucl. Sci. **49**, 2440 (2002)
12. Arnaboldi, C., et al.: Phys. Lett. B **557**, 167 (2003). doi:10.1016/S0370-2693(03)00212-0
13. Rodin, V.A., Faessler, A., Šimkovic, F., Vogel, P.: Nucl. Phys. A **766**, 107 (2006). doi: 10.1016/j.nuclphysa.2005.12.004
14. Rodin, V.A., Faessler, A., Šimkovic, F., Vogel, P.: (2007). 0706.4304v1 [nucl-th]
15. Kortelainen, M., Suhonen, J.: Phys. Rev. C **76**, 024315 (2007). 0708.0115 [nucl-th]
16. Menendez, J., Poves, A., Caurier, E., Nowacki, F.: (2008)

http://www.springer.com/978-94-007-1231-7

Model of the Response Function of CUORE Bolometers
Vignati, M.
2011, XII, 107 p., Hardcover
ISBN: 978-94-007-1231-7